Exact non-Markovian dynamics of qubits coupled to two interacting environments

H. Z. Shen,[1,2] D. X. Li,[1] Shi-Lei Su,[3] Y. H. Zhou,[4] and X. X. Yi[1,2,*]

[1]*Center for Quantum Sciences and School of Physics, Northeast Normal University, Changchun 130024, China*

[2]*Center for Advanced Optoelectronic Functional Materials Research, and Key Laboratory for UV Light-Emitting Materials and Technology of Ministry of Education, Northeast Normal University, Changchun 130024, China*

[3]*School of Physical Science and Engineering and Key Laboratory of Materials Physics of Ministry of Education of China, Zhengzhou University, Zhengzhou 450052, China*

[4]*College of Physics and Electronic Information, Baicheng Normal University, Baicheng 137000, China*

(Received 22 January 2017; revised manuscript received 11 July 2017; published 5 September 2017)

As the memory effect may be helpful in quantum information processing, non-Markovian dynamics plays an important role in the description of many-body open systems. Among these topics, the system consisting of independent qubits interacting with several coupled environments is of particular interest. In this paper, we study the exact non-Markovian dynamics of two independent qubits. Each of the qubits interacts individually with its environment, and these two environments coupled with each other. We investigate the non-Markovianity measure of the system for the whole parameter regime without the rotating-wave approximation (RWA) and compare the results with that under the RWA. We find that the non-Markovianity measure for two qubits manifests a transition from a non-Markovian to Markovian regime regardless of the coupling strength between the environments. The physical origin of this transition is revealed, and a possible observation of the prediction in superconducting quantum interference devices is discussed.

DOI: 10.1103/PhysRevA.96.033805

I. INTRODUCTION

The dynamics of open quantum system is a long-standing problem [1]. In recent years, with the rapid development of quantum information technology [2,3], the role played by open quantum system has become more and more interesting. Generally speaking, all realistic quantum systems are open due to the unavoidable couplings to environment (of memory or memoryless) [4–7]. A memoryless environment leads to Markovian dynamics, while another results in non-Markovian dynamics. The non-Markovian dynamics proves to be useful in quantum information processing including quantum state engineering, quantum control, and quantum channel capacity [7–11]. Non-Markovianity can be characterized by the information flow between the system and its environment [12–17], leading to different measures of non-Markovianity [18–23]. There are many factors that can influence the non-Markovian dynamics, such as the strength of system-environment coupling, the structure of the environment, temperature, system-environment correlations in the initial state [24–28], etc.

In the traditional researches, people in general focus on the quantum system coupled to a single environment, which has been investigated theoretically [29–42] and experimentally [43–49]. However, in the real world, there might be a situation of many environments coupling to a system simultaneously [50–52]. For example, in a quantum dot the electron spin may be affected strongly by the surrounding nuclei [51,53]. The neighbor nitrogen impurities constitute the principal bath for a nitrogen-vacancy center, while the carbon-13 nuclear spins may also couple to them [50]. A similar situation also occurs for a single-donor electron spin in silicon [52,54]. Motivated by these facts [50–54], some efforts have been devoted to studying the effects of multiple environments on the dynamics of an open system [55–58]. In the treatments of composite environments, the interaction between these environments was not taken into account. This gives rise to a question of how the environment-environment coupling affects the non-Markovian feature of the open system. The answer to this question would be useful for engineering and controlling quantum memories for applications in theory [59–61] and in experiments [62–64].

In this paper, we will study the exact non-Markovian dynamics of two independent qubits induced by the coupling between two environments, which can be realized in superconducting quantum interference devices (SQUIDs) [64,65]. We will show that non-Markovian dynamics can be observed in the whole parameter regime of the system. Because the rotating-wave approximation (RWA) holds only in the weak system-environment coupling limit, the non-RWA effects are necessarily taken into account in the studies of non-Markovianity. Under the RWA, we analyze non-Markovianity with different parameters. We discuss the transition from non-Markovian to Markovian regime and compare the difference between the results with RWA and without RWA in the non-Markovianity [44]. The physical origin of transition from non-Markovian to Markovian regime is also revealed. Finally, we study how the parameters, such as the coupling strength between the environments, influence the non-Markovianity in the strong coupling regime.

The remainder of this paper is as follows. In Sec. II we introduce the system and take the RWA to describe the system. Then we analytically derive an exact dynamics for the first qubit of two independent qubits coupled to two coupled environments. In Sec. III we examine the situation of the nonrotating wave approximation and compare the results with that given by the RWA. Discussion and conclusions are presented in Sec. IV.

*yixx@nenu.edu.cn

II. DYNAMICS

In this section, we first present a model to describe the system under study, whose dynamics is believed to be non-Markovian due to the coupling between the environments. This system can be realized by circuit quantum electrodynamics involving superconducting quantum interference devices (SQUIDs), multimode cavities, and superconducting qubits. We derive the interaction Hamiltonian in the interaction picture, assuming the system and its environment are in the initial density matrix being factorized into a direct product of the system and the environment state. In this case, we study the non-Markovianity measure in the rotating-wave approximation (RWA) for the coupling between the composite environments.

A. Model Hamiltonian

To begin, we consider the dephasing dynamics of the coupling between the composite environments, in which two decoupled-qubits are interacting with their own environment, respectively,

$$\hat{H} = \hat{H}_0 + \hat{H}_I, \hat{H}_0 = \hat{H}_S + \hat{H}_J + \hat{H}_E, \tag{1}$$

where

$$\begin{aligned}
&\hat{H}_S = \hbar\nu_1\hat{\sigma}_1^z + \hbar\nu_2\hat{\sigma}_2^z, \hat{H}_E = \sum_{k=1}^{\infty}\hbar\omega_k\hat{b}_k^\dagger\hat{b}_k + \sum_{k=1}^{\infty}\hbar\Omega_k\hat{a}_k^\dagger\hat{a}_k,\\
&\hat{H}_J = \hbar J(\hat{a}_1 + \hat{a}_1^\dagger)(\hat{b}_1 + \hat{b}_1^\dagger),\\
&\hat{H}_I = \hat{\sigma}_1^z\sum_{k=1}^{\infty}\hbar g_k(\hat{b}_k + \hat{b}_k^\dagger) + \hat{\sigma}_2^z\sum_{k=1}^{\infty}\hbar G_k(\hat{a}_k + \hat{a}_k^\dagger),
\end{aligned} \tag{2}$$

where $\hat{H}_S$ is free Hamiltonian of the decoupled qubits with the frequencies ν_1 and ν_2, respectively. $\hat{H}_E$ is the environments Hamiltonian with frequencies ω_k and Ω_k. $\hat{H}_I$ is the Hamiltonian of two qubits subjected to the two environments with the coupling strength g_k and G_k. $\hat{a}_k$ ($\hat{a}_k^\dagger$) and $\hat{b}_k$ ($\hat{b}_k^\dagger$) denote the annihilation (creation) operators of the kth mode of the two environments, respectively. $\hat{\sigma}_1^z$ and $\hat{\sigma}_2^z$ denote the Pauli operators for the qubits, respectively. J is the coupling strength between the composite environments. The derivation of the Hamiltonian (1) is given in Appendix A, which can be realized by applying a circuit quantum electrodynamics via SQUIDs.

Equation (1) is critical for the rest of the paper, which describes the model of two qubits coupled to the composite environments. Each of the two qubits interacts locally with its own environment, and the coupling between the composite environments is realized by the SQUIDs. This is comparable to previous researches regarding the nonlocal memory effects [60,66–69], in which the composite environments are decoupled under the initial environment-environment correlations.

B. Exact non-Markovian dynamics for the system with RWA

The interaction Hamiltonian $\hat{H}_J$ of in Eq. (1) contains the counter-rotating terms $\hat{a}_1\hat{b}_1$ and $\hat{a}_1^\dagger\hat{b}_1^\dagger$. A widely used approximation in quantum optics and quantum information communities is the rotating-wave approximation, which is valid in the following conditions:

$$\Omega_1 + \omega_1 \gg J, \tag{3}$$

$$|\Omega_1 - \omega_1| \ll \Omega_1 + \omega_1, \tag{4}$$

where Eq. (3) holds true in the weak-coupling limit with respect to the sum of eigenfrequencies of the two environments. The second condition (4) requires two frequencies to be near resonance. Derivation of Eqs. (3) and (4) can be found in Appendix B. Then under this condition, $\hat{H}_J$ in Eq. (1) can be written as

$$\hat{H}_J^{RWA} = \hbar J(\hat{a}_1\hat{b}_1^\dagger + \hat{b}_1\hat{a}_1^\dagger). \tag{5}$$

The dynamics of the total system density matrix in the interaction picture is obtained from the Schrödinger equation:

$$\frac{d}{dt}\rho_T(t) = -\frac{i}{\hbar}[\hat{H}_I(t), \rho_T(t)]. \tag{6}$$

The total density matrix of the total system at time t is formally given by

$$\rho_T(t) = U(t)\rho_T(0)U^\dagger(t), \tag{7}$$

where $\rho_T(0)$ is the initial density matrix of the total system. The time-evolution operator is

$$U(t) = \mathcal{T}\exp\left[-\frac{i}{\hbar}\int_0^t ds\hat{H}_I(s)\right], \tag{8}$$

where the notation $\mathcal{T}$ represents the time-ordered product, which orders any product of superoperators such that the time argument increases from right to left. The interaction Hamiltonian in interaction picture can be defined as

$$\hat{H}_I(t) = e^{\frac{i}{\hbar}\hat{H}_0 t}\hat{H}_I e^{-\frac{i}{\hbar}\hat{H}_0 t}. \tag{9}$$

Simple algebra yields

$$\begin{aligned}
\hat{H}_I(t) = \Big\{&\left[\hbar g_1 D(t)\hat{\sigma}_1^z + G_1 A(t)\hat{\sigma}_2^z\right]\hat{a}_1\\
&+\left[\hbar g_1 C(t)\hat{\sigma}_1^z + G_1 B(t)\hat{\sigma}_2^z\right]\hat{b}_1\\
&+\hbar\sum_{k=2}^{\infty} g_k e^{-i\omega_k t}\hat{\sigma}_1^z\hat{b}_k + G_k e^{-i\Omega_k t}\hat{\sigma}_2^z\hat{a}_k\Big\} + \text{H.c.},
\end{aligned} \tag{10}$$

where H.c. stands for Hermitian conjugate. The time-dependent coefficients $A(t)$, $B(t)$, $C(t)$, and $D(t)$ can be found in Appendix C. Based on Eq. (10), we calculate the commutation relation for the Hamiltonian at time t and t',

$$\begin{aligned}
\hat{h}(t,t') &\equiv [\hat{H}_I(t), \hat{H}_I(t')]\\
&= \hbar^2\phi_1(t-t') + 2i\hbar^2\hat{\sigma}_1^z\hat{\sigma}_2^z S(t-t'),
\end{aligned} \tag{11}$$

where $\phi_1(t-t') = |g_1|^2[D(t)D^*(t') - D(t')D^*(t) + C(t)C^*(t') - C(t')C^*(t)] + |G_1|^2[A(t)A^*(t') - A(t')A^*(t) + B(t)B^*(t') - B(t')B^*(t)] - 2i\sum_{k=2}[|g_k|^2\sin\omega_k(t-t') + |G_k|^2\sin\Omega_k(t-t')]$ and $S(t-t') = g_1G_1\text{Im}[D^*(t')A(t) + D(t)A^*(t') + B(t)C^*(t') + B^*(t')C(t)]$. The commutation relation is a function only dependent on the difference of time t and t', and c.c. denotes complex conjugate. The second term

in Eq. (11) describes the effective coupling induced by the interaction between the composite environments. This means that the Hamiltonian at any time τ, $\hat{H}_I(\tau)$, commutes with Eq. (11). In other words, we can obtain the identity

$$[\hat{H}_I(\tau),\hat{h}(t,t')] = 0. \tag{12}$$

Resorting to the Magnus expansion [70,71] of the exponent of $U(t) = \exp[\hat{\Omega}(t)]$ in Eq. (8), we write the three first terms of that series:

$$\begin{aligned}\hat{\Omega}(t) = &-\frac{i}{\hbar}\int_0^t \hat{H}_I(t_1)\,dt_1 - \frac{1}{2\hbar^2}\int_0^t dt_1\int_0^{t_1} dt_2\hat{h}(t_1,t_2)\\ &+\frac{i}{6\hbar^3}\int_0^t dt_1\int_0^{t_1} dt_2\int_0^{t_2} dt_3\{[\hat{H}_I(t_1),\hat{h}(t_2,t_3)]\\ &+[\hat{H}_I(t_3),\hat{h}(t_2,t_1)]\} + \cdots.\end{aligned} \tag{13}$$

Collecting all together, we can exactly calculate the time evolution operator to be

$$U(t) = e^{-\frac{i}{\hbar}\int_0^t dt_1\hat{H}_I(t_1)}e^{-\frac{1}{2\hbar^2}\int_0^t dt_1\int_0^{t_1} dt_2\hat{h}(t_1,t_2)}. \tag{14}$$

Substituting Eq. (11) into the above equation, we can obtain

$$U(t) = \chi(t)e^{-i\int_0^t dt_1\hat{H}_I(t_1) - iS_1(t)\hat{\sigma}_1^z\hat{\sigma}_2^z}, \tag{15}$$

where

$$\begin{aligned}S_1(t) =& \int_0^t dt_1\int_0^{t_1} dt_2 S(t_1-t_2),\\ \chi(t) =& e^{-\frac{1}{2}\int_0^t dt_1\int_0^{t_1} dt_2\phi_1(t_1-t_2)}.\end{aligned} \tag{16}$$

We find that $S_1(t)$ and $\chi(t)$ are all the functions only dependent on time t. Then Eq. (15) can be further rewritten as

$$\begin{aligned}U(t) = &\chi(t)e^{\frac{1}{2}(d_1\hat{a}_1 - d_1^*\hat{a}_1^\dagger)\hat{\sigma}_1^z}e^{\frac{1}{2}\sum_{k=1}^{\infty}(\alpha_k\hat{a}_k-\alpha_k^*\hat{a}_k^\dagger)\hat{\sigma}_2^z}\\ &\times e^{\frac{1}{2}(\lambda_1\hat{b}_1-\lambda_1^*\hat{b}_1^\dagger)\hat{\sigma}_2^z}e^{\frac{1}{2}\sum_{k=1}^{\infty}(c_k\hat{b}_k-c_k^*\hat{b}_k^\dagger)\hat{\sigma}_1^z}e^{i\frac{1}{2}\Theta(t)\hat{\sigma}_1^z\hat{\sigma}_2^z},\end{aligned} \tag{17}$$

where $\Theta(t) = 2p_1(t) + 2p_2(t) - S_1(t)$ with $p_1(t) = \mathrm{Im}[\frac{1}{4}\alpha_1^*(t)d_1(t)]$ and $p_2(t) = \mathrm{Im}[\frac{1}{4}c_1^*(t)\lambda_1(t)]$, $c_k(t) = g_k(-i2\int_0^t dt_1 e^{-i\omega_k t_1})$, $\alpha_k(t) = G_k(-i2\int_0^t dt_1 e^{-i\Omega_k t_1})$ at $k \geqslant 2$, and

$$\begin{aligned}\alpha_1(t) =& G_1[-i2\int_0^t dt_1 A(t_1)],\\ d_1(t) =& g_1[-i2\int_0^t dt_1 D(t_1)],\\ c_1(t) =& g_1[-i2\int_0^t dt_1 C(t_1)],\\ \lambda_1(t) =& G_1[-i2\int_0^t dt_1 B(t_1)].\end{aligned} \tag{18}$$

Note that the preexponential factor $\chi(t)$ in Eq. (17) can be considered as the correction term due to the time-ordering operation. The first and third exponential factors denote the influence of the first mode of each environment on the interaction Hamiltonian, the second and the fourth terms are a dephasing effect induced by the composite environments. The final term is that the coupling between the composite environments leads to the indirect coupling of two qubits.

To proceed, we assume that the initial state of the composite environments is a product of vacuums of the two environments. This assumption is reasonable when the thermal relaxation time scale $\sim \hbar/k_BT$ is very small compared with time scale of the system, e.g., that characterized by the coupling strength $1/J$. Further, in order to study the influence of the interaction between the two environments on the non-Markovian dynamics, we assume that the initial density matrix is a product of the system and the environment state,

$$\rho_T(0) = \rho(0)\otimes\rho_B, \tag{19}$$

where $\rho_S(0) = \rho_1(0)\otimes\rho_2(0)$ with the states of the two qubits $\hat{\sigma}_z|0\rangle = -|0\rangle$, $\hat{\sigma}_z|1\rangle = |1\rangle$. The initial states for two qubits might take a general form $\rho_1(0) = \rho_{11}^{(1)}(0)|1\rangle_1\langle 1| + \rho_{10}^{(1)}(0)|1\rangle_1\langle 0| + \rho_{01}^{(1)}(0)|0\rangle_1\langle 1| + \rho_{00}^{(1)}(0)|0\rangle_1\langle 0|$, and $\rho_2(0) = (1-\eta)|1\rangle_2\langle 1| + \rho_{10}(0)|1\rangle_2\langle 0| + \rho_{01}|0\rangle_2\langle 1| + \eta|0\rangle_2\langle 0|$, in which $\rho_{11}(0)|1\rangle_1\langle 1|$ denotes a state with the first qubit being in the excited state $|0\rangle_1$ with the probability $\rho_{11}(0)$. The other states have similar notations. $\rho_B = \rho_{B1}\otimes\rho_{B2}$ is the initial vacuum with $\rho_{Bj} = |0\rangle_j\langle 0|$, where $j = 1,2$, i.e., the two environments are vacuum states, respectively. Hence the reduced density matrix elements in the interaction picture can be written as by tracing over the composite environments:

$$\rho_{mn,rs}(t) = \langle mn|\mathrm{Tr}_B[U(t)\rho(0)\otimes\rho_B U^\dagger(t)]|rs\rangle, \tag{20}$$

where $\rho_{mn,rs}(t) \equiv \langle mn|\rho|rs\rangle$ with $(m,n,r,s = 1,0)$. Substituting Eq. (17) into Eq. (20), we can obtain

$$\begin{aligned}\rho_{mn,rs}(t) = &a_{mn}a_{rs}^* e^{\frac{1}{2}i\Theta(t)(-1)^{m+n} - \frac{1}{2}i\Theta(t)(-1)^{r+s}}\\ &\times \mathrm{Tr}_{B_2}(e^{\frac{1}{2}(\lambda_1\hat{b}_1-\lambda_1^*\hat{b}_1^\dagger)(-1)^{n+1}}e^{\frac{1}{2}\sum_k(c_k\hat{b}_k-c_k^*\hat{b}_k^\dagger)(-1)^{m+1}}\\ &\times e^{-\frac{1}{2}\sum_k(c_k\hat{b}_k-c_k^*\hat{b}_k^\dagger)(-1)^{r+1}}e^{-\frac{1}{2}(\lambda_1\hat{b}_1-\lambda_1^*\hat{b}_1^\dagger)(-1)^{s+1}}\rho_{B_2})\\ &\times \mathrm{Tr}_{B_1}(e^{\frac{1}{2}(d_1\hat{a}_1-d^*\hat{a}_1^\dagger)(-1)^{m+1}}e^{\frac{1}{2}\sum_k(\alpha_k\hat{a}_k-\alpha_k^*\hat{a}_k^\dagger)(-1)^{n+1}}\\ &\times e^{-\frac{1}{2}\sum_k(\alpha_k\hat{a}_k-\alpha_k^*\hat{a}_k^\dagger)(-1)^{s+1}}e^{-\frac{1}{2}(d_1\hat{a}_1-d_1^*\hat{a}_1^\dagger)(-1)^{r+1}}\rho_{B_1}).\end{aligned} \tag{21}$$

Then exact reduced density matrix of the first qubit with an initial state $\rho_1(0)$ (in matrix form) can be evaluated as

$$\rho_1(t) = \begin{pmatrix}\rho_{11}^{(1)}(0) & \rho_{10}^{(1)}(0)R(t)e^{-F(t)}\\ \rho_{01}^{(1)}(0)R^*(t)e^{-F(t)} & \rho_{00}^{(1)}(0)\end{pmatrix} \tag{22}$$

with

$$\begin{aligned}F(t) = &[0.5|c_1(t)|^2 + 0.5|d_1(t)|^2 - 8g_1^2\sin^2(\omega_1 t/2)/\omega_1^2\\ &+4\int_0^\infty d\omega G(\omega)(1-\cos\omega t)]\end{aligned} \tag{23}$$

and

$$R(t) = r(t)e^{i\theta(t)}, \tag{24}$$

where $\theta(t) = \arctan[(1-2\eta)\tan\Theta(t)]$, $r(t) = \sqrt{\cos^2\Theta(t) + (2\eta-1)^2\sin^2\Theta(t)}$, and $c_1(t)$, $\lambda_1(t)$, $d_1(t)$, and $\alpha_1(t)$ are given by Eq. (18). From the point of view of the first qubit, the rest of the Hamiltonian except the first qubit (two environments, interaction between them, the second qubit) is regarded as the external environments. Therefore the intrinsic parameters of the environment as well as interaction

between two environments all affect the non-Markovian dynamics of the first qubit. The effective spectral function reads

$$G(\omega) = \frac{J(\omega)}{\omega^2}, \tag{25}$$

with $J(\omega) = \sum_k |g_k|^2 \delta(\omega - \omega_k)$ being the reservoir spectral density. In particular, in the continuum limit, we have

$$J(\omega) = \frac{\gamma \Pi \mathcal{M}^2}{2} \int_0^\infty dk \frac{\omega_k \sin^2(\Lambda k)}{\omega_k^2 + (\gamma/2)^2} \delta(\omega - \omega_k), \tag{26}$$

where $\mathcal{M} = E_J \frac{S\pi\mu_0}{2\pi r \phi_0} \sqrt{\frac{\hbar}{lL}} \sin(\pi\Phi/\phi_0)$ is a parameter measuring the qubit-environment coupling, and $\omega_k = Xk, X = \pi/l\sqrt{LC}, \Lambda = \pi x/l$. We use the dephasing dynamics (22) for the first qubit to study measure the degree of non-Markovianity. The trace distance between two reduced states evolved through Eq. (22) is given by

$$\mathcal{D}(t, \rho_S^{1,2}) = \sqrt{\Delta_p^2 + |\Delta_c|^2 r^2(t) e^{-2F(t)}},$$

where $\Delta_p = \rho_{11}^{(1)}(0) - \rho_{11}^{(2)}(0)$ and $\Delta_c = \rho_{10}^{(1)}(0) - \rho_{10}^{(2)}(0)$ are the differences between, respectively, the populations and the coherences of the two initial conditions ρ_S^1 and ρ_S^2 for the first qubit. The couple of initial states that maximizes the growth of the trace distance for the dephasing model (22) is given by the pure orthogonal states $\rho_S^{1,2} = |\psi_\pm\rangle\langle\psi_\pm|$, where $|\psi_\pm\rangle = \frac{1}{\sqrt{2}}(|1\rangle_1 \pm |0\rangle_1)$ (for more details, please see Refs. [12–15]). This leads to $\Delta_p = 0$ and $|\Delta_c| = 1$, which corresponds to trace distance $\mathcal{D}(t, \rho_S^{1,2}) = r(t)e^{-F(t)}$. Therefore the measure of non-Markovianity reads

$$\mathcal{N} = \int_{F'(t)<r'(t)/r(t)} d[r(t)e^{-F(t)}], \tag{27}$$

where the integration is over all intervals in which $F'(t) < r'(t)/r(t)$. $F'(t)$ and $r'(t)$ denote derivative of functions $F(t)$ and $r(t)$, respectively.

C. Non-Markovianity for the system in the composite environments

In Fig. 1 we show decoherence factor as a function of time for different Ω_1. The blue dashed line corresponds to $J = 0$, and the red line corresponds to $J = 1$. We can find that there is a period compared to the case where only the first qubit couples with the first environment ($J = 0$, corresponding to blue dashed line). This means that memory effects are present with these types of environments, and the decoherence factors are nonmonotonic, allowing recoherence effects to occur in the system of interest. In addition, in all cases, we show decoherence factor possesses a "dip," which makes the behavior of the decoherence factor reach its minimum. The strength and location of the dip is determined by the environment parameters.

Solving integral equation (26), we can obtain the analytical expression for the spectrum density

$$J(\omega) = \frac{\gamma \Pi \mathcal{M}^2}{2X} \frac{\omega \sin^2(\Lambda\omega/X)}{\omega^2 + (\gamma/2)^2}. \tag{28}$$

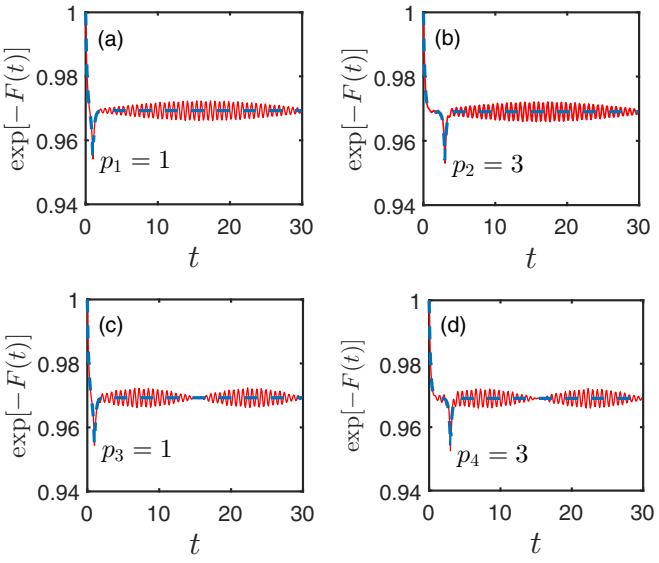

FIG. 1. Decoherence factor as a function of the time for different J. It can be seen that specially appointed areas (see points $p_1 - p_4$) present an anomalous decoherence behavior in the decoherence factor leading to recoherence effects. The blue dashed line corresponds to $J = 0$, and the red line corresponds to $J = 1$. Here and hereafter, X, $\mathcal{M}$, g_1, ω_1, Ω_1, and γ are rescaled in units of E_J, and t is then in units of $1/E_J$. For the sake of simplicity, in the posterior part of the paper we take the second qubit to be in the ground state, i.e., $\eta = 1$, which leads to $r(t) \equiv 1$ in Eq. (24), and $R(t) = e^{i\theta(t)}$. Parameters chosen are $X = 0.4$, $\mathcal{M} = 0.2$, $g_1 = 0.2$, $\omega_1 = 10$, $\gamma = 10$, $\Pi = 0.1$, $\Lambda = 0.2$, $\Omega_1 = 15$ for (a), $\Lambda = 0.6$, $\Omega_1 = 15$ for (b), $\Lambda = 0.2$, $\Omega_1 = 12$ for (c), $\Lambda = 0.6$, $\Omega_1 = 12$ for (d).

Substituting Eq. (28) into Eq. (23), we can obtain the analytical solution for the case of $J = 0$,

$$\begin{aligned} F(t) &\equiv 4 \int_0^\infty d\omega G(\omega)(1 - \cos\omega t)] \\ &= \frac{\pi \Pi \mathcal{M}^2}{16X} [\sigma(t) + e^{-0.5\gamma(t+2\mathrm{T})} + e^{-0.5\gamma|t-2T|}], \end{aligned} \tag{29}$$

where $= \Lambda/X, \sigma(t) = 2 - 2e^{-T\gamma} - 2e^{-t\gamma/2}$. From Eq. (29), we find the exponential factor in $F(t)$ has an special point at $2T$, which determines the position of the collapse point in Fig. 1 (i.e., point p_1: $2T = 2\Lambda/X = 1$; point p_2: $2T = 3$; point p_3: $2T = 1$; point p_4: $2T = 3$]. In Fig. 2 we plot the non-Markovianity $\mathcal{N}$ as a function of the coupling strength J between the two environments in the RWA. As shown in the figure, the system exhibits non-Markovian dynamics, judged by $\mathcal{N} \neq 0$, increase until the coupling strength is above a certain threshold. In general, non-Markovianity increases with qubit-environment interaction g_1 for a fixed coupling strength J. The non-Markovianity measure increases very fast and approaches a maximum with a very small change in the coupling strength J, and then it decays asymptotically to a saturated value. This indicates that when coupling between the composite environments reaches a critical value, the non-Markovianity shows a large flow of information from the environment to its system. In addition, we find that

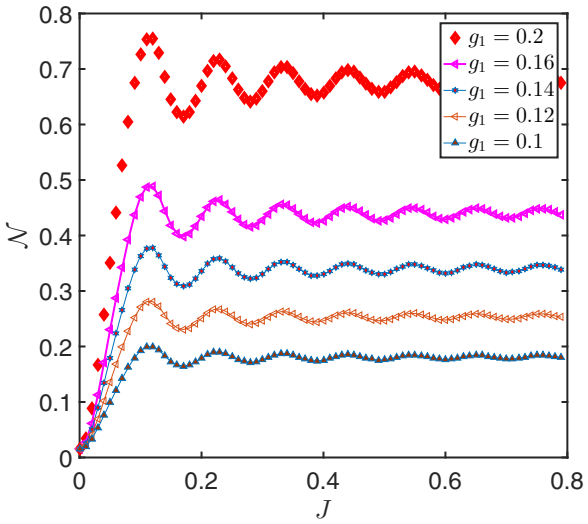

FIG. 2. Non-Markovianity measure $\mathcal{N}$ as a function of the coupling strength J between two environments in the weak coupling regime (RWA). Parameters chosen are $X = 0.4$, $\mathcal{M} = 0.2$, $\eta = 1$, $\omega_1 = 5.1$, $\Omega_1 = 5$, $\gamma = 10$, $\Pi = 0.1$, $\Lambda = 0.2$.

non-Markovianity measure increases as the coupling of qubit environemnt g_1 increase for a fixed coupling between the composite environments. This quantity gives a bound on the maximum rate at which quantum information can be reliably transmitted along a noisy quantum channel, and it is therefore of key importance in the design of noise-robust quantum advanced devices [72–75].

III. SITUATION WITHOUT ROTATING WAVE APPROXIMATION

We start by showing that if the weak coupling between the two environments is used, a good approximation for the value of the non-Markovianity measure can be obtained. When the RWA breaks down, we must consider the influence of the counter-rotating terms between the two environments on the non-Markovianity. In the strong coupling regime (regime A and regime B in Fig. 8), Eq. (5) becomes

$$\hat{H}_J = \hbar J(\hat{a}_1^\dagger + \hat{a}_1)(\hat{b}_1^\dagger + \hat{b}_1). \tag{30}$$

In Eq. (30), the coupling between the composite environments due to the overlapping for two modes of the composite environments, is written in its full form without performing the rotating wave approximation, which can be obtained with SQUIDs [65,76]. In order to calculate Eq. (9), we need to obtain the following analytical relation by means of the Heisenberg picture method:

$$e^{\frac{i}{\hbar}\hat{H}_0 t}\hat{a}_1 e^{-\frac{i}{\hbar}\hat{H}_0 t} = N(t)\hat{a}_1 + M(t)\hat{a}_1^\dagger + N_1(t)\hat{b}_1 + M_1(t)\hat{b}_1^\dagger, \tag{31}$$

where the time-dependent coefficients $N(t)$ and $M(t)$ can be determined with the integro-differential equation

$$\begin{aligned}\frac{d}{dt}N(t) &= -i\Omega_1 N(t) - \int_0^t d\tau[N(\tau) + M^*(\tau)]\kappa(t-\tau),\\ \frac{d}{dt}M(t) &= -i\Omega_1 M(t) - \int_0^t d\tau[N^*(\tau) + M(\tau)]\kappa(t-\tau),\end{aligned} \tag{32}$$

where

$$\kappa(\tau) = -2iJ^2\sin(\omega_1\tau). \tag{33}$$

By means of a Laplace transform to Eq. (32), we easily obtain the analytical solution of $N(t)$ and $M(t)$ due to Eq. (32) being two coupled linear integro-differential equations. After solving $N(t)$ and $M(t)$, $N_1(t)$ and $M_1(t)$ can be given by

$$\begin{aligned}N_1(t) &= -iJ\int_0^t d\tau e^{-i\omega_1\tau}[N(t-\tau) - M(t-\tau)],\\ M_1(t) &= -iJ\int_0^t d\tau e^{i\omega_1\tau}[N(t-\tau) - M(t-\tau)].\end{aligned} \tag{34}$$

Similarly, the result of $e^{iH_0 t}\hat{b}_1 e^{-iH_0 t}$ can be given by

$$e^{\frac{i}{\hbar}\hat{H}_0 t}\hat{b}_1 e^{-\frac{i}{\hbar}\hat{H}_0 t} = Q_1(t)\hat{a}_1 + P_1(t)\hat{a}_1^\dagger + Q(t)\hat{b}_1 + P(t)\hat{b}_1^\dagger, \tag{35}$$

where $Q(t)$ and $P(t)$ are given by

$$\begin{aligned}\frac{d}{dt}Q(t) &= -i\omega_1 Q(t) - \int_0^t d\tau[Q(\tau) + P^*(\tau)]\kappa_1(t-\tau),\\ \frac{d}{dt}P(t) &= -i\omega_1 P(t) - \int_0^t d\tau[Q^*(\tau) + P(\tau)]\kappa_1(t-\tau),\end{aligned} \tag{36}$$

where

$$\kappa_1(\tau) = -2iJ^2\sin(\Omega_1\tau). \tag{37}$$

Making a Laplace transform to Eq. (32), we analytically obtain $Q(t)$ and $P(t)$ so that $Q_1(t)$ and $P_1(t)$ can be given by

$$\begin{aligned}Q_1(t) &= -iJ\int_0^t d\tau e^{-i\Omega_1\tau}[Q(t-\tau) - P(t-\tau)],\\ P_1(t) &= -iJ\int_0^t d\tau e^{i\Omega_1\tau}[Q(t-\tau) - P(t-\tau)].\end{aligned} \tag{38}$$

Therefore, substituting Eqs. (31) and (35) into Eq. (9), we can obtain the same result as Eq. (10) in the non-RWA with the replacement

$$\begin{aligned}A(t) &\to N(t) + M^*(t),\\ B(t) &\to N_1(t) + M_1^*(t),\\ C(t) &\to Q(t) + P^*(t),\\ D(t) &\to Q_1(t) + P_1^*(t).\end{aligned} \tag{39}$$

In order to compare the results of the RWA process with that of the non-RWA one, we plot decoherence factor for the system as a function of time t with the change from the weak (RWA) to strong coupling regime (non-RWA) in Fig. 3. From the figure we find that the decoherence factors $\exp[-F(t)]$ given

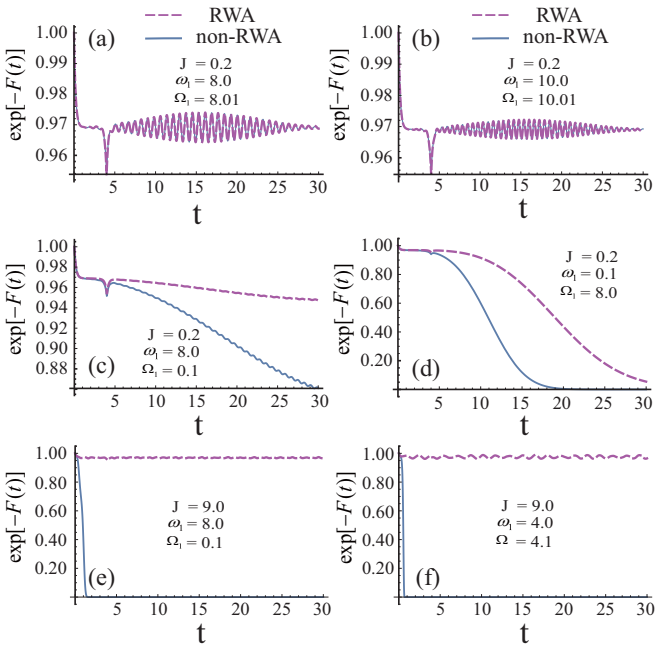

FIG. 3. Decoherence factor for two decoupled qubits interacting with the composite environments as a function of time t with the change from the weak (RWA; see regime C in Fig. 8) to a strong coupling regime (non-RWA; see regimes A and B in Fig. 8). The solid lines describe the situations in non-RWA [see Eq. (30)], and the dashed lines describe the situations in the RWA [see Eq. (5)]. The other parameters chosen are $X = 0.4$, $\mathcal{M} = 0.2$, $\eta = 1$, $g_1 = 0.2$, $\omega_1 = 10$, $\gamma = 10$, $\Pi = 0.1$, $\Lambda = 0.2$, $\Omega_1 = 11$.

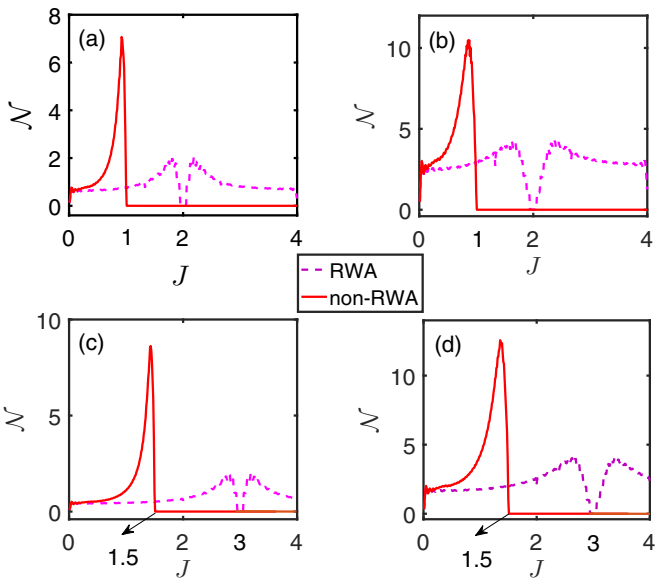

FIG. 4. Non-Markovianity measure $\mathcal{N}$ as a function of the coupling strength J in a nonrotating wave regime. Here we set $\omega_e \equiv \omega_1 = \Omega_1$. The parameters chosen are $X = 0.4$, $\mathcal{M} = 0.2$, $\eta = 1$, $\gamma = 10$, $\Pi = 0.1$, $\Lambda = 0.2$, $g_1 = 0.1$, $\omega_e = 2$ for (a), $g_1 = 0.2$, $\omega_e = 2$ for (b), $g_1 = 0.1$, $\omega_e = 3$ for (c), $g_1 = 0.2$, $\omega_e = 3$ for (d). We find the non-Markovianity for RWA drops to zero at point $J = \omega_e$ and later revives as the parameter J continues to grow. However, for the case of non-RWA (the strong-coupling regime), non-Markovianity measures are identically zero at $J \geqslant 0.5\omega_e$.

by the RWA are in good agreement with those obtained by the exact non-RWA when the conditions for RWA are satisfied [see panels (a) and (b) in Fig. 3]. When the detuning tunes large [see panels (c) and (d) in Fig. 3] or coupling strength becomes strong [see panels (e) and (f) in Fig. 3], the curve obtained by the RWA has large deviations from those obtained by the exact non-RWA. This is due to that the counter-rotating terms $J\hat{a}_1\hat{b}_1 e^{-it(\omega_1+\Omega_1)} + \text{H.c.}$ can be neglected when the conditions $J \ll \omega_1 + \Omega_1$ and $|\Omega_1 - \omega_1| \ll \Omega_1 + \omega_1$ are simultaneously satisfied in the interaction picture.

Thus, the surprising message is that a stronger memory effect of the environment may be helpful in enhancing the non-Markovianity measure of the system due to the presence of the strong coupling between the composite environments. In fact, because one environment is only a part of the composite environments now, an integrated consideration including both the qubits and the environments is needed to determine the non-Markovian character of the qubits of interest. The memory effect from the composite environments exhibits several interesting features of non-Markovianity measure in the strong coupling regime as demonstrated in the following.

To shed more light on the effect of the non-RWA between the composite environments on the non-Markovianity measure $\mathcal{N}$ as a function of J, we compare the results of non-RWA with those in the case of RWA identified clearly in Fig. 4 in the strong coupling regime between the composite environments. The red lines and purple dashed lines correspond to the non-RWA regime and RWA regime, respectively. When J becomes finite and keeps increasing, the non-Markovianity measure of the system increases, and one might expect the memory effects of the environment to enhance the amount of information backflow, and hence to increase the non-Markovianity as well. We can see non-Markovianity measure has a simple monotonic relation with J, in which the RWA and non-RWA agree well with each other when $J < J_c$ in weak coupling regime ($J_c \ll \omega_e$). A common nonmonotonic behavior of the non-Markovianity for the RWA and non-RWA is presented when $J > J_c$; the non-Markovianity first increases with increasing J, and after it reaches a maximum value, it decreases with further increasing of J. The obviously distinct phenomenon is that at $J = \omega_e$, the non-Markovianity for RWA drops to zero and later revives as the parameter J continues to grow. However, for the case of non-RWA (the strong-coupling regime), non-Markovianity measures are identically zero at $J \geqslant 0.5\omega_e$ (see Fig. 4). In other words, the transition points from Markovian dynamics to non-Markovian dynamics for RWA and non-RWA are equal to the frequency ω_e and $0.5\omega_e$ of the first mode for the environments, respectively. The phenomenon of transition can arise from the fact that the coupling strength J between the composite environments becomes so strong that the qubits have disturbed the environment, thereby undermining the foundation of the Markovian approximation, which eventually results in the appearance of information backflow to the system.

To further demonstrate our results, we directly investigate the trace distance $\mathcal{D}(t, \rho_S^{1,2}) = \exp[-F(t)]$. Figure 5 shows its evolution when the coupling strength between the composite

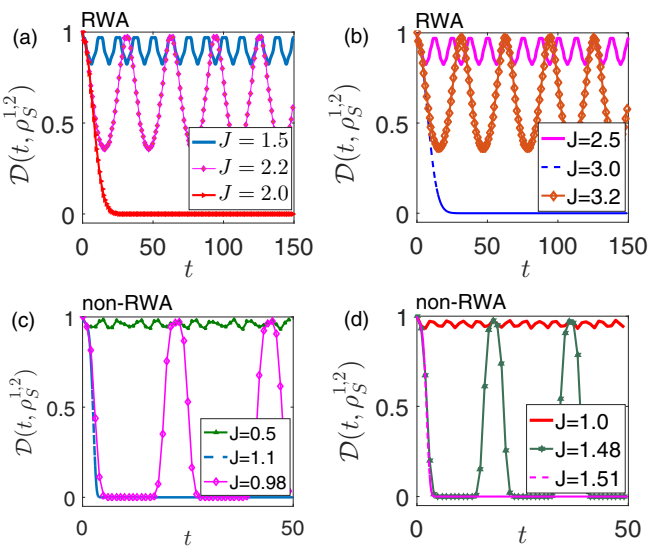

FIG. 5. The trace distance $\mathcal{D}(t,\rho_S^{1,2})$ as a function of time for three different values of the coupling between the composite environments. Parameters of Figs. 5(a) and 5(c) are the same as the purple dashed and red line in Fig. 4(a), respectively. Parameters of Figs. 5(b) and 5(d) are the same as the purple dashed and red line in Fig. 4(c), respectively.

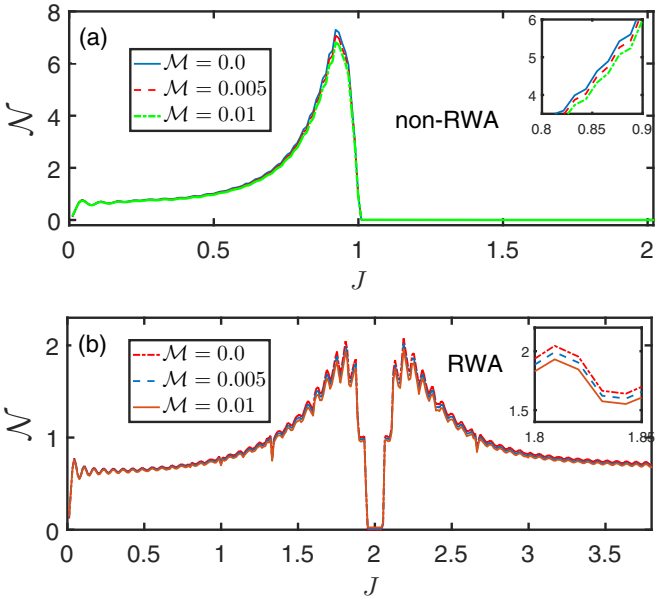

FIG. 6. Non-Markovianity measure $\mathcal{N}$ as a function of J in nonrotating wave regime with three different qubit-environment strengths, $\mathcal{M}=0$, $\mathcal{M}=0.005$, and $\mathcal{M}=0.01$. Parameters chosen are the same as Fig. 4(a); panels (a) and (b) correspond to the red line (non-RWA) and the purple dashed line (RWA) in Fig. 4(a), respectively. The physical origin of the transition of non-Markovianity measure from Markovian to non-Markovian dynamics under the non-RWA and RWA, respectively, is shown.

environments takes interesting special points with fixed coupling strength $\mathcal{M}=0.2$, which explains the interesting phenomena of Fig. 4. Parameters of Figs. 5(a) and 5(c) are the same as Fig. 4(a) with $\omega_e=2$, while parameters of Figs. 5(b) and 5(d) are the same as Fig. 4(c) with $\omega_e=3$. We now discuss (a) and (c) in Fig. 5. We choose three discrete points from the continuous points of the coupling strength in Fig. 4, for RWA: $J=1.5$, $J=2.0$, and $J=2.2$, while for non-RWA: $J=0.5$, $J=0.98$, and $J=1.1$, respectively. These points pass through the regime transitions non-Markovian ($J<\omega_e$) $\xrightarrow{J=\omega_e}$ Markovian $\xrightarrow{J>\omega_e}$ non-Markovian as J increases, i.e., the trace distance $\mathcal{D}(t,\rho_S^{1,2})$ is not monotonic and exhibits oscillations, so that the evolution is non-Markovian for $J=1.5$ and $J=2.2$ [see Fig. 5(a)], while the trace distance $\mathcal{D}(t,\rho_S^{1,2})$ becomes monotonic and asymptotically decays to zero for $J=2.0$ [see Fig. 5(a)]; therefore the evolution process becomes Markovian dynamics. Similar to the RWA process, in the non-RWA one, a notable point is that even in the non-Markovian regime, $\mathcal{D}(t,\rho_S^{1,2})$ exhibits different patterns for different J. When $J=0.5\omega_e$, the curve of $\mathcal{D}(t,\rho_S^{1,2})$ is oscillatory. However, for the case $J=0.98\omega_e$, $\mathcal{D}(t,\rho_S^{1,2})$ keeps hitting the zero line, as seen in Fig. 5(c). These zero points mean that the two states ρ_1 and ρ_2 are totally indistinguishable at those time points and correspond to the points where $\mathcal{D}(t,\rho_S^{1,2})=0$. The qubits actually evolve into their ground state at these zero points and hence lose all the information. The qubits are supposed to stop evolving after this point without recapturing the lost information under a typical Markovian evolution. Thus, the bounce of $\mathcal{D}(t,\rho_S^{1,2})$ serves as a remarkably non-Markovian feature, meaning that the information could flow back into the qubits even if it has been completely leaked into the environment, which would never happen in a Markovian evolution. The similar observations can be found in Figs. 5(b) and 5(d).

In Fig. 6, we can further reveal the physical origin of the transition of the non-Markovianity measure from Markovian to non-Markovian dynamics under the non-RWA [Fig. 6(a)] and RWA [Fig. 6(b)], which corresponds to Fig. 4(a). For the case of non-RWA in Fig. 6(a), we find that non-Markovianity measure has a finite value when we consider only the two first modes of each environment, i.e., $\mathcal{M}=0$ be equivalent to $g_k=G_k=0$ at $k\geqslant 2$ except $g_1\neq 0, G_1\neq 0$ (see the blue line in Fig. 6). As $\mathcal{M}$ increases, the non-Markovianity measure decreases (see the red dashed and green dotted lines in Fig. 6). When $\mathcal{M}$ crosses a critical value, the non-Markovian measure decays to zero [see Fig. 4(a)], where $\mathcal{M}=0.01$. For the case of RWA in Fig. 6(b), it has a similar observation to non-RWA. This means that there are two mechanisms of information backflow to work: (1) the excitation exchange induced by the coupling between the composite environments and (2) the dephasing effects between the qubits and the environments. The competition between the two effects determines the non-Markovianity. The non-Markovianity measure will increase when the former plays the dominating role, otherwise, the non-Markovianity measure will decrease.

IV. CONCLUSION

In this paper, we have investigated the exact non-Markovian dynamics of two independent qubits coupling with several

coupled environments. The non-Markovianity is induced by the coupling between environments that couple to the two qubits simultaneously. We find that the non-Markovian dynamics can be observed in the whole parameter regimes of the system. The study has been performed not only in the rotating-wave approximation (RWA) but also in the non-RWA. The results suggest that the system dynamics can be controlled by tuning the coupling between the environments. Transitions from non-Markovian to Markovian regimes have been identified [44], and the physical origin of the transition have been found. These features are independent of the nature of the environments, but are closely related to the coupling between the environments. It is worth addressing that our system is the minimal model to show these effects clearly, and it is feasible within current experimental technologies in circuit QED [64,65,77].

ACKNOWLEDGMENTS

The authors thank the anonymous referee for constructive comments that helped to improve the quality of this paper. H.Z.S. would like to thank Prof. S. Felicetti for valuable discussions. This work is supported by the National Natural Science Foundation of China (NSFC) under Grants No. 11534002, No. 61475033, No. 11775048, and No. 11705025, China Postdoctoral Science Foundation under Grants No. 2016M600223 and No. 2017T100192, Subject Construction Project of School of Physics of Northeast Normal University under Grant No. 111715014, and the Fundamental Research Funds for the Central Universities under Grant No. 2412017QD005.

APPENDIX A: THE MODEL HAMILTONIAN DERIVED BY SUPERCONDUCTOR CIRCUIT QED

The schematic diagram of the setup used in our scheme is shown in Fig. 7, which consists of a small superconducting box with excess Cooper-pair charges, formed by a SQUID with capacitance C_J and Josephson coupling energy E_J, pierced by an external magnetic flux Φ. A control gate voltage V_g is connected to the system via a gate capacitor C_g. The Hamiltonian of the system is

$$\hat{H} = \hbar E_c(n-\bar{n})^2 - \hbar E_J \cos\varphi_1 - \hbar E_J \cos\varphi_2, \quad \text{(A1)}$$

where n is the number operator of (excess) Cooper-pair charges on the box, $E_c = 2e^2/(C_g + 2C_J)/\hbar$ is the charging energy, $\bar{n} = C_g V_g/2e$ is the induced charge controlled by the gate voltage V_g and φ_m, and $(m = 1,2)$ is the gauge-invariant phase difference between the two sides of the mth junction. We here focus on the charging regime where $E_c \gg E_J$. In this case, a convenient basis is formed by the charge states, parametrized by the number of Cooper pairs n on the box with its conjugate ϕ; they satisfy the standard commutation relation $[\phi,n] = i$. At temperatures much lower than the charging energy and restricting the gate charge to the range of $\bar{n} \in [0,1]$, only a pair of adjacent charge states $|0\rangle,|1\rangle$ on the island is relevant. The Hamiltonian $(A1)$ is then reduced to [64,78–81]

$$\hat{H}_1 = -\hbar E_{ce}\hat{\sigma}_z - \hbar E(\Phi)\hat{\sigma}_x, \quad \text{(A2)}$$

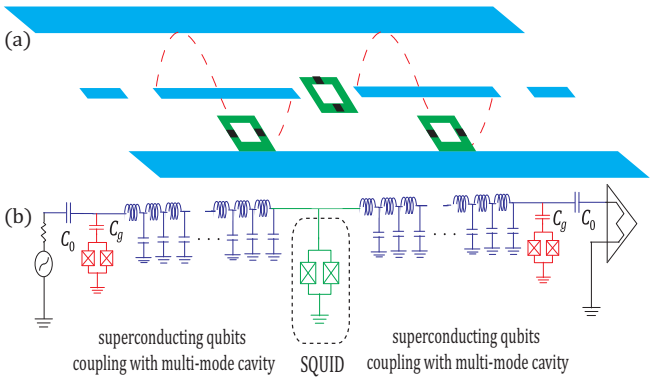

FIG. 7. (a) The 1D transmission line resonator consists of a full-wave section of a superconducting coplanar waveguide. A Cooper-pair box qubit is placed between the superconducting lines and is capacitively coupled to the voltage standing wave, yielding a strong electric dipole interaction between the qubit and photon in the cavity. The two setups can be grounded through a SQUID. The blue lines represent two parallel strip lines of isolating material, where the superconducting region between them constitutes the coplanar waveguide. Each multimode-cavity interacts with a superconductor qubit that is denoted by a red regime. This scheme can be realized by circuit QED [64,65]. (b) Circuit diagram for the previous scheme, where the cavities are effectively represented by LC resonators. We assume two identical Josephson junctions of the SQUID with effective Josephson energy by an external flux Φ, and superconductor qubits are constituted by two Josephson junctions shunted by a large capacitance.

where $E_{ce} = 2E_c(1-2\bar{n})/\hbar, E(\Phi) = E_J\cos(\pi\Phi/\phi_0)/\hbar$ with $\phi_0 = h/2e$ being flux quanta, and $\hat{\sigma}_z$ and $\hat{\sigma}_x$ are the Pauli matrices.

When a superconducting qubit is placed superconductor transmission line resonator, the total magnetic flux generated by the resonator and SQUID penetrating the qubit loop is given by classical magnetic flux and magnetic flux in a lossy superconductor transmission line resonator:

$$\Phi' = \Phi + \Phi_q, \quad \text{(A3)}$$

where

$$\Phi_q = \sum_k c_k(\hat{a}_k + \hat{a}_k^\dagger), \quad \text{(A4)}$$

where $c_k = S_o\frac{\Gamma_k\mu_0}{2\pi r_1}\sqrt{\frac{\hbar\omega_k}{lL}}\sin(k\pi x/l)$. $\Gamma_k = \sqrt{\Pi(\gamma/2)/[\omega_k^2 + (\gamma/2)^2]}$ is proportional to a Lorentzian shape with γ being the decay rate of a quasimode of cavity, Π the bandwidth associated with the cavity wall transparency [82]. S_o is the area surrounded by the superconducting quantum interference device loop, and r_1 is the distance between the superconducting quantum interference device and transmission lines [64]. x is the position of the qubit penetrating the superconductor transmission line resonator. μ_0 $(= 4\pi \times 10^{-7} Hm^{-1})$ is the magnetic permeability in vacuum. $\omega_k = v\pi k/l$ $(v = 1/\sqrt{LC}$ is the propagation velocity) is the quantized frequency of the superconductor harmonic cavity with $L(C)$ the total inductance (capacitance) of the stripline. Then total quantized Hamiltonian can be

rewritten as ($\Phi \to \Phi'$)

$$\hat{H}_1 = -\hbar E_{ce}\hat{\sigma}_z - \hbar E_J \cos[\pi(\Phi + \Phi_q)/\phi_0]\hat{\sigma}_x. \quad \text{(A5)}$$

Generally speaking, $\Phi_q \ll \Phi$, and in the degeneracy point $\bar{n} = 1/2$ leading to $E_{ce} = 0$ [78,80], then the Hamiltonian (A5) approximately reads

$$\hat{H}_1 = -\hbar E(\Phi)\hat{\sigma}_x + \sum_k \hbar\omega_k \hat{a}_k^\dagger \hat{a}_k - \sum_k \hbar G_k(\hat{a}_k + \hat{a}_k^\dagger)\hat{\sigma}_x, \quad \text{(A6)}$$

where the coupling strength $G_k = E_J c_k \frac{\Phi}{\phi_0}\sin(\pi\Phi/\phi_0)$.

Now we consider the coupling of two superconducting qubits coupling with multimode cavity, which can be implemented by means of a SQUID. The coupling of first-mode for each cavity with the eigenfrequency ω_1 and Ω_1 can be realized by matching the frequency first mode for each cavity and the frequency ω of the ac magnetic flux for the SQUID [65,83]

$$\hat{H}_J = \hbar J(\hat{a}_1 + \hat{a}_1^\dagger)(\hat{b}_1 + \hat{b}_1^\dagger), \quad \text{(A7)}$$

where the SQUID driven by external fluxes allows a modulation of the electrical boundary condition of the cavities and their interaction, which can tune the interaction between the resonators and their boundary conditions, provided the modulation frequency is smaller than the SQUID plasma frequency [65,83]. In addition, two qubits interacting at the same time with two multimode cavities, respectively,

$$\hat{H}' = \hat{H}'_0 + \hat{H}'_I, \hat{H}'_0 = \hat{H}'_S + \hat{H}'_E, \quad \text{(A8)}$$

where

$$\begin{aligned}
\hat{H}'_S &= \hbar\nu_1\hat{\sigma}_1^x + \hbar\nu_2\hat{\sigma}_2^x,\\
\hat{H}'_E &= \sum_{k=1}^{\infty}\hbar\omega_k\hat{b}_k^\dagger\hat{b}_k + \sum_{k=1}^{\infty}\hbar\Omega_k\hat{a}_k^\dagger\hat{a}_k,\\
\hat{H}'_I &= -\hat{\sigma}_1^x\sum_{k=1}^{\infty}\hbar g_k(\hat{b}_k + \hat{b}_k^\dagger) - \hat{\sigma}_2^x\sum_{k=1}^{\infty}\hbar G_k(\hat{a}_k + \hat{a}_k^\dagger),
\end{aligned} \quad \text{(A9)}$$

where the parameters $\nu_1 = -E_1(\Phi_1)$, $\nu_2 = -E_2(\Phi_2)$, $g_k = E_J c_{1,k}\frac{\Phi_1}{\phi_0}\sin(\pi\Phi_1/\phi_0)$, $G_k = E_J c_{2,k}\frac{\Phi_2}{\phi_0}\sin(\pi\Phi_2/\phi_0)$. Finally, we can obtain the Hamiltonian (1) by the unitary transform to $\hat{H} = e^{\hat{S}}(\hat{H}' + \hat{H}_J)e^{-\hat{S}}$, where the generator of the transform is $\hat{S} = -i\pi\hat{\sigma}_1^y/4 - i\pi\hat{\sigma}_2^y/4$.

APPENDIX B: CONDITION FOR ROTATING WAVE APPROXIMATION

In this section, we give the justification about the conditions of rotating wave approximation as follows. We take the Hamiltonian for two coupled environments (first-mode) as a non-RWA form

$$\hat{H} = \hat{H}_0 + \hat{H}_J \quad \text{(B1)}$$

with

$$\hat{H}_0 = \hbar\Omega_1\hat{a}_1^\dagger\hat{a}_1 + \hbar\omega_1\hat{b}_1^\dagger\hat{b}_1, \quad \text{(B2)}$$

$$\hat{H}_J = \hbar J(\hat{a}_1 + \hat{a}_1^\dagger)(\hat{b}_1 + \hat{b}_1^\dagger), \quad \text{(B3)}$$

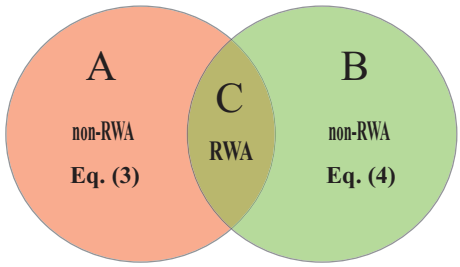

FIG. 8. Comparison of rotating wave approximation (corresponding to regime C) and nonrotating wave approximation [corresponding to regime A given by Eq. (3) and regime B given by Eq. (4)].

where J denotes the coupling strength between two environments with their own eigenfrequency Ω_1 and ω_1, and $\hat{a}_1$ and $\hat{b}_1$ stand for annihilation operators of the environment. In the interaction picture, we have

$$\hat{H}_J(t) = \hbar J\hat{a}_1\hat{b}_1^\dagger e^{-i(\Omega_1-\omega_1)t} + \hbar J\hat{a}_1\hat{b}_1 e^{-i(\Omega_1+\omega_1)t} + \text{H.c.} \quad \text{(B4)}$$

The time evolution operator is given by

$$\begin{aligned}
U(t) &= \mathcal{T}\exp[-\frac{i}{\hbar}\int_0^t \hat{H}_J(t_1)\,dt_1]\\
&= 1 - \frac{i}{\hbar}\int_0^t \hat{H}_J(t_1)\,dt_1 - \frac{1}{\hbar^2}\int_0^t dt_1\\
&\quad\times\int_0^{t_1}\hat{H}_J(t_1)\hat{H}_J(t_2)\,dt_2 + \cdots.
\end{aligned} \quad \text{(B5)}$$

Substituting Eq. (B4) into Eq. (B5), we obtain

$$\begin{aligned}
-\frac{i}{\hbar}\int_0^t \hat{H}_J(t_1)\,dt_1 &= \frac{J}{\Omega_1-\omega_1}(e^{-i(\Omega_1-\omega_1)t} - 1)\hat{a}_1\hat{b}_1^\dagger\\
&\quad - \frac{J}{\Omega_1-\omega_1}(e^{i(\Omega_1-\omega_1)t} - 1)\hat{b}_1\hat{a}_1^\dagger\\
&\quad + \frac{J}{\Omega_1+\omega_1}(e^{-i(\Omega_1+\omega_1)t} - 1)\hat{a}_1\hat{b}_1\\
&\quad - \frac{J}{\Omega_1+\omega_1}(e^{i(\Omega_1+\omega_1)t} - 1)\hat{b}_1^\dagger\hat{a}_1^\dagger.
\end{aligned} \quad \text{(B6)}$$

The RWA requires

$$\begin{cases}\frac{J}{\Omega_1+\omega_1} \ll 1,\\ \frac{J}{|\Omega_1-\omega_1|} \gg \frac{J}{\Omega_1+\omega_1},\end{cases} \quad \text{(B7)}$$

which leads to the conditions (3) and (4) for RWA (see regime C in Fig. 8). In this case, the counter-rotating terms can be neglected.

When the system parameters do not satisfy Eq. (B7) (see regimes A and B in Fig. 8), we cannot neglect the counter-rotating terms in Hamiltonian (B4), therefore this RWA is broken down. In this case, we must consider the influence of counter-rotating terms on the system dynamics.

APPENDIX C: THE DERIVATION OF EQ. (10)

In Eq. (9), the operator a_1 in the interaction picture can be rewritten as

$$e^{\frac{i}{\hbar}\hat{H}_0 t}\hat{a}_1 e^{-\frac{i}{\hbar}\hat{H}_0 t}, \tag{C1}$$

in accordance with the formula

$$\begin{aligned} e^{\hat{x}}\hat{y}e^{-\hat{x}} &= \hat{y} + [\hat{x},\hat{y}] + \frac{1}{2!}[\hat{x},[\hat{x},\hat{y}]]\cdots \\ &\quad + \frac{1}{n!}[\underbrace{\hat{x},[\hat{x}\cdots[\hat{x}}_{n\ \hat{x}},\hat{y}]]] + \cdots \\ &\equiv [\hat{x}^{(0)},\hat{y}] + \cdots \frac{1}{n!}[\hat{x}^{(n)},\hat{y}] + \cdots; \end{aligned} \tag{C2}$$

here we set $\hat{x} = \hat{H}_0$ and $\hat{y} = \hat{a}_1$, and we can obtain the commutation relation,

$$\begin{aligned} \left[\hat{H}_0^{(1)},\hat{a}_1\right] &= -\Omega_1\hat{a}_1 - J\hat{b}_1 \equiv A_1\hat{a}_1 + B_1\hat{b}_1, \ldots \\ \left[\hat{H}_0^{(n)},\hat{a}_1\right] &= A_n\hat{a}_1 + B_n\hat{b}_1, \end{aligned} \tag{C3}$$

where we can write the recurrence relation as the form of matrix,

$$r_{n+1} = M^n r_1, \tag{C4}$$

with the Hermitian matrix $M = \begin{pmatrix} -\omega_1 & -J \\ -J & -\Omega_1 \end{pmatrix}$ as well as $r_n = \begin{pmatrix} B_n \\ A_n \end{pmatrix}$. The eigenvalues of M are

$$E_m = -\frac{1}{2}(\omega_1 + \Omega_1) + \eta\cos(\pi m), \tag{C5}$$

where

$$\begin{aligned} \eta &= \frac{1}{2}\sqrt{4J^2 - 2\omega_1\Omega_1 + \omega_1^2 + \Omega_1^2}, \\ \cos(\theta) &= \frac{\Omega_1 - \omega_1}{2\eta}, \\ \sin(\theta) &= \frac{|J|}{\eta}. \end{aligned} \tag{C6}$$

The corresponding eigenstates are

$$\phi_m = \begin{pmatrix} a_m \\ \beta_m \end{pmatrix}, \tag{C7}$$

where

$$\begin{aligned} \alpha_m &= -\sin\left(\frac{\theta m + 2\pi}{2m}\right), \\ \beta_m &= \cos\left[\frac{\theta + (1-m)\pi}{2}\right]. \end{aligned} \tag{C8}$$

Inserting the complete basis of M into Eq. (C4), we can get

$$\begin{pmatrix} B_{n+1} \\ A_{n+1} \end{pmatrix} = E_1^n \begin{pmatrix} |a_1|^2 & a_1\beta_1^* \\ a_1^*\beta_1 & |\beta_1|^2 \end{pmatrix} r_1 + E_2^n \begin{pmatrix} |a_2|^2 & a_2\beta_2^* \\ a_2^*\beta_2 & |\beta_2|^2 \end{pmatrix} r_1, \tag{C9}$$

which leads to

$$\begin{aligned} B_n &= \sum_{j=1,2} E_j^n |a_j|^2 \frac{B_1}{E_j} + E_j^n a_j\beta_j^* \frac{A_1}{E_j}, \\ A_n &= \sum_{j=1,2} E_j^n a_j^*\beta_j \frac{B_1}{E_j} + E_j^n |\beta_j|^2 \frac{A_1}{E_j}. \end{aligned} \tag{C10}$$

In conclusion, we make use of Eq. (C2) and Eq. (C10) to rewrite Eq. (C1) as

$$\begin{aligned} &e^{\frac{i}{\hbar}\hat{H}_0 t}\hat{a}_1 e^{-\frac{i}{\hbar}\hat{H}_0 t} \\ &= \hat{a}_1\left\{1 + A_1 it + \frac{A_2(it)^2}{2} + \cdots + \frac{A_n(it)^n}{n!} + \ldots\right\} \\ &\quad + \hat{b}_1\left\{B_1 it + \frac{B_2(it)^2}{2} + \cdots + \frac{B_n(it)^n}{n!} + \ldots\right\}. \end{aligned} \tag{C11}$$

Simple algebra yields

$$e^{\frac{i}{\hbar}\hat{H}_0 t}\hat{a}_1 e^{-\frac{i}{\hbar}\hat{H}_0 t} = A(t)\hat{a}_1 + B(t)\hat{b}_1, \tag{C12}$$

where

$$\begin{aligned} A(t) &= 1 + \sum_{j=1,2}\left(e^{iE_j t} - 1\right)\left[a_j^*\beta_j\frac{B_1}{E_j} + \left(|\beta_j|\right)^2\frac{A_1}{E_j}\right], \\ B(t) &= \sum_{j=1,2}\left(e^{iE_j t} - 1\right)\left(|a_j|^2\frac{B_1}{E_j} + a_j\beta_j^*\frac{A_1}{E_j}\right). \end{aligned} \tag{C13}$$

Similarly, the operator b_1 in the interaction picture can be obtained easily, which can be summarized as

$$e^{\frac{i}{\hbar}\hat{H}_0 t}\hat{b}_1 e^{-\frac{i}{\hbar}\hat{H}_0 t} = C(t)\hat{b}_1 + D(t)\hat{a}_1, \tag{C14}$$

where

$$\begin{aligned} C(t) &= 1 + \sum_{j=1,2}\left(e^{iE_j t} - 1\right)\left(|a_j|^2\frac{C_1}{E_j} + a_j\beta_j^*\frac{D_1}{E_j}\right), \\ D(t) &= \sum_{j=1,2}\left(e^{iE_j t} - 1\right)\left(a_j^*\beta_j\frac{C_1}{E_j} + |\beta_j|^2\frac{D_1}{E_j}\right), \end{aligned} \tag{C15}$$

where $C_1 = -\omega_1$ and $D_1 = -J$. Considering Eqs. (C12) and (C15), we can obtain Eq. (10).

[1] H. P. Breuer and F. Petruccione, *Theory of Open Quantum Systems* (Oxford University Press, New York, 2002).

[2] M. Nielsen and I. Chuang, *Quantum Computation and Quantum Information* (Cambridge University Press, Cambridge, 2000).

[3] T. D. Ladd, F. Jelezko, R. Laflamme, Y. Nakamura, C. Monroe, and J. L. O'Brien, Quantum computers, Nature (London) **464**, 45 (2010).

[4] J. G. Li, J. Zou, and B. Shao, Non-Markovianity of the damped Jaynes-Cummings model with detuning, Phys. Rev. A **81**, 062124 (2010).

[5] C. W. Gardiner and P. Zoller, *Quantum Noise* (Springer-Verlag, Berlin, 2000).

[6] R. Lo Franco, B. Bellomo, S. Maniscalco, and G. Compagno, Dynamics of quantum correlations in two-qubit systems within

non-Markovian environments, Int. J. Mod. Phys. B **27**, 1345053 (2013).
[7] F. Caruso, V. Giovannetti, C. Lupo, and S. Mancini, Quantum channels and memory effects, Rev. Mod. Phys. **86**, 1203 (2014).
[8] A. D'Arrigo, R. Lo Franco, G. Benenti, E. Paladino, and G. Falci, Recovering entanglement by local operations, Ann. Phys. **350**, 211 (2014).
[9] R. Lo Franco, A. D'Arrigo, G. Falci, G. Compagno, and E. Paladino, Preserving entanglement and nonlocality in solid-state qubits by dynamical decoupling, Phys. Rev. B **90**, 054304 (2014).
[10] B. Bylicka, D. Chruściński, and S. Maniscalco, Non-Markovianity and reservoir memory of quantum channels: A quantum information theory perspective, Sci. Rep. **4**, 5720 (2014).
[11] S. B. Xue, R. B. Wu, W. M. Zhang, J. Zhang, C. W. Li, and T. J. Tarn, Decoherence suppression via non-Markovian coherent feedback control, Phys. Rev. A **86**, 052304 (2012).
[12] H. P. Breuer, E. M. Laine, J. Piilo, and B. Vacchini, *Colloquium*: Non-Markovian dynamics in open quantum systems, Rev. Mod. Phys. **88**, 021002 (2016).
[13] H. P. Breuer, E. M. Laine, and J. Piilo, Measure for the Degree of Non-Markovian Behavior of Quantum Processes in Open Systems, Phys. Rev. Lett. **103**, 210401 (2009).
[14] E. M. Laine, J. Piilo, and H. P. Breuer, Measure for the non-Markovianity of quantum processes, Phys. Rev. A **81**, 062115 (2010).
[15] C. Addis, B. Bylicka, D. Chruściński, and S. Maniscalco, Comparative study of non-Markovianity measures in exactly solvable one- and two-qubit models, Phys. Rev. A **90**, 052103 (2014).
[16] S. Wißmann, A. Karlsson, E. M. Laine, J. Piilo, and H. P. Breuer, Optimal state pairs for non-Markovian quantum dynamics, Phys. Rev. A **86**, 062108 (2012).
[17] S. Wißmann, H. P. Breuer, and B. Vacchini, Generalized trace-distance measure connecting quantum and classical non-Markovianity, Phys. Rev. A **92**, 042108 (2015).
[18] S. Lorenzo, F. Plastina, and M. Paternostro, Geometrical characterization of non-Markovianity, Phys. Rev. A **88**, 020102(R) (2013).
[19] Á. Rivas, S. F. Huelga, and M. B. Plenio, Entanglement and Non-Markovianity of Quantum Evolutions, Phys. Rev. Lett. **105**, 050403 (2010).
[20] S. L. Luo, S. S. Fu, and H. T. Song, Quantifying non-Markovianity via correlations, Phys. Rev. A **86**, 044101 (2012).
[21] M. M. Wolf, J. Eisert, T. S. Cubitt, and J. I. Cirac, Assessing Non-Markovian Quantum Dynamics, Phys. Rev. Lett. **101**, 150402 (2008).
[22] X. M. Lu, X. G. Wang, and C. P. Sun, Quantum Fisher information flow and non-Markovian processes of open systems, Phys. Rev. A **82**, 042103 (2010).
[23] D. Chruściński and S. Maniscalco, Degree of Non-Markovianity of Quantum Evolution, Phys. Rev. Lett. **112**, 120404 (2014).
[24] Á. Rivas, S. F. Huelga, and M. B. Plenio, Quantum non-Markovianity: Characterization, quantification and detection, Rep. Prog. Phys. **77**, 094001 (2014).
[25] E. M. Laine, J. Piilo, and H. P. Breuer, Witness for initial system-environment correlations in open-system dynamics, Europhys. Lett. **92**, 60010 (2010).
[26] J. Dajka and J. Łuczka, Distance growth of quantum states due to initial system-environment correlations, Phys. Rev. A **82**, 012341 (2010).
[27] A. Smirne, H. P. Breuer, J. Piilo, and B. Vacchini, Initial correlations in open-systems dynamics: The Jaynes-Cummings model, Phys. Rev. A **82**, 062114 (2010).
[28] Z. X. Man, A. Smirne, Y. J. Xia, and B. Vacchini, Quantum interference induced by initial system-environment correlations, Phys. Lett. A **376**, 2477 (2012).
[29] M. Schlosshauer, The quantum-to-classical transition and decoherence, arXiv:1404.2635 (2014).
[30] I. d. Vega and D. Alonso, Dynamics of non-Markovian open quantum systems, Rev. Mod. Phys. **89**, 015001 (2017).
[31] F. Verstraete, M. M. Wolf, and J. I. Cirac, Quantum computation and quantum-state engineering driven by dissipation, Nat. Phys. **5**, 633 (2009).
[32] M. J. Kastoryano, M. M. Wolf, and J. Eisert, Precisely Timing Dissipative Quantum Information Processing, Phys. Rev. Lett. **110**, 110501 (2013).
[33] S. C. Hou, S. L. Liang, and X. X. Yi, Non-Markovianity and memory effects in quantum open systems, Phys. Rev. A **91**, 012109 (2015).
[34] H. Z. Shen, X. Q. Shao, G. C. Wang, X. L. Zhao, and X. X. Yi, Quantum phase transition in a coupled two-level system embedded in anisotropic three-dimensional photonic crystals, Phys. Rev. E **93**, 012107 (2016).
[35] H. Z. Shen, M. Qin, and X. X. Yi, Single-photon storing in coupled non-Markovian atom-cavity system, Phys. Rev. A **88**, 033835 (2013).
[36] H. Z. Shen, D. X. Li, and X. X. Yi, Non-Markovian linear response theory for quantum open systems and its applications, Phys. Rev. E **95**, 012156 (2017).
[37] D. Chruściński and A. Kossakowski, Non-Markovian Quantum Dynamics: Local Versus Nonlocal, Phys. Rev. Lett. **104**, 070406 (2010).
[38] J. S. Xu, C. F. Li, M. Gong, X. B. Zou, C. H. Shi, G. Chen, and G. C. Guo, Experimental Demonstration of Photonic Entanglement Collapse and Revival, Phys. Rev. Lett. **104**, 100502 (2010).
[39] A. W. Chin, S. F. Huelga, and M. B. Plenio, Quantum Metrology in Non-Markovian Environments, Phys. Rev. Lett. **109**, 233601 (2012).
[40] S. Deffner and E. Lutz, Quantum Speed Limit for Non-Markovian Dynamics, Phys. Rev. Lett. **111**, 010402 (2013).
[41] A. J. Leggett, S. Chakravarty, A. T. Dorsey, M. P. A. Fisher, A. Garg, and W. Zwerger, Dynamics of the dissipative two-state system, Rev. Mod. Phys. **59**, 1 (1987).
[42] U. Weiss, *Quantum Dissipative Systems*, 3rd ed. (World Scientific Press, Singapore, 2008).
[43] S. Gröblacher, A. Trubarov, N. Prigge, G. D. Cole, M. Aspelmeyer, and J. Eisert, Observation of non-Markovian micromechanical Brownian motion, Nat. Commun. **6**, 7606 (2015).
[44] B. H. Liu, L. Li, Y. F. Huang, C. F. Li, G. C. Guo, E. M. Laine, H. P. Breuer, and J. Piilo, Experimental control of the transition from Markovian to non-Markovian dynamics of open quantum systems, Nat. Phys. **7**, 931 (2011).
[45] U. Hoeppe, C. Wolff, J. Küchenmeister, J. Niegemann, M. Drescher, H. Benner, and K. Busch, Direct Observation of

Non-Markovian Radiation Dynamics in 3D Bulk Photonic Crystals, Phys. Rev. Lett. **108**, 043603 (2012).

[46] J.-S. Xu, X.-Y. Xu, C.-F. Li, C.-J. Zhang, X.-B. Zou, and G.-C. Guo, Experimental investigation of classical and quantum correlations under decoherence, Nat. Commun. **1**, 7 (2010).

[47] J. S. Xu, C. F. Li, C. J. Zhang, X. Y. Xu, Y. S. Zhang, and G. C. Guo, Experimental investigation of the non-Markovian dynamics of classical and quantum correlations, Phys. Rev. A **82**, 042328 (2010).

[48] K. H. Madsen, S. Ates, T. Lund-Hansen, A. Löffler, S. Reitzenstein, A. Forchel, and P. Lodahl, Observation of Non-Markovian Dynamics of a Single Quantum Dot in a Micropillar Cavity, Phys. Rev. Lett. **106**, 233601 (2011).

[49] A. Orieux, A. D'Arrigo, G. Ferranti, R. Lo Franco, G. Benenti, E. Paladino, G. Falci, F. Sciarrino, and P. Mataloni, Experimental on-demand recovery of entanglement by local operations within non-Markovian dynamics, Sci. Rep. **5**, 8575 (2015).

[50] R. Hanson, V. V. Dobrovitski, A. E. Feiguin, O. Gywat, and D. D. Awschalom, Coherent dynamics of a single spin interacting with an adjustable spin bath, Science **320**, 352 (2008).

[51] R. Hanson, L. P. Kouwehoven, J. R. Petta, S. Tarucha, and L. M. K. Vandersypen, Spins in few-electron quantum dots, Rev. Mod. Phys. **79**, 1217 (2007).

[52] J. J. Pla, K. Y. Tan, J. P. Dehollain, W. H. Lim, J. J. L. Morton, D. N. Jamieson, A. S. Dzurak, and A. Morello, A single-atom electron spin qubit in silicon, Nature (London) **489**, 541 (2012).

[53] E. A. Chekhovich, M. N. Makhonin, A. I. Tartakovskii, A. Yacoby, H. Bluhm, K. C. Nowack, and L. M. K. Vandersypen, Nuclear spin effects in semiconductor quantum dots, Nat. Mater. **12**, 494 (2013).

[54] A. M. Tyryshkin, S. Tojo, J. J. L. Morton, H. Riemann, N. V. Abrosimov, P. Becker, H. J. Pohl, T. Schenkel, M. L. W. Thewalt, K. M. Itoh, and S. A. Lyon, Electron spin coherence exceeding seconds in high-purity silicon, Nat. Mater. **11**, 143 (2012).

[55] T. J. G. Apollaro, S. Lorenzo, C. Di Franco, F. Plastina, and M. Paternostro, Competition between memory-keeping and memory-erasing decoherence channels, Phys. Rev. A **90**, 012310 (2014); C. K. Chan, G. D. Lin, S. F. Yelin, and M. D. Lukin, Quantum interference between independent reservoirs in open quantum systems, *ibid.* **89**, 042117 (2014); Z. X. Man, N. B. An, and Y. J. Xia, Non-Markovianity of a two-level system transversally coupled to multiple bosonic reservoirs, *ibid.* **90**, 062104 (2014); Z. X. Man, Y. J. Xia, and R. Lo Franco, Harnessing non-Markovian quantum memory by environmental coupling, *ibid.* **92**, 012315 (2015); A. Z. Chaudhry and J. B. Gong, Decoherence induced by a composite environment, *ibid.* **89**, 014104 (2014).

[56] T. Ma, Y. Chen, T. Chen, S. R. Hedemann, and T. Yu, Crossover between non-Markovian and Markovian dynamics induced by a hierarchical environment, Phys. Rev. A **90**, 042108 (2014).

[57] A. Fruchtman, B. W. Lovett, S. C. Benjamin, and E. M. Gauger, Quantum dynamics in a tiered non-Markovian environment, New J. Phys. **17**, 023063 (2015).

[58] C. Addis, G. Brebner, P. Haikka, and S. Maniscalco, Coherence trapping and information backflow in dephasing qubits, Phys. Rev. A **89**, 024101 (2014).

[59] N. Qiu and X. B. Wang, Fast creation of entanglement by interaction with a common bath, Phys. Rev. A **88**, 062332 (2013).

[60] S. Wißmann and H. P. Breuer, Role of entanglement for nonlocal memory effects, Phys. Rev. A **90**, 032117 (2014).

[61] R. Mengoni, L. Memarzadeh, and S. Mancini, Entanglement from dissipative dynamics into overlapping environments, Phys. Rev. A **90**, 062341 (2014).

[62] A. Chiuri, C. Greganti, L. Mazzola, M. Paternostro, and P. Mataloni, Linear optics simulation of quantum non-Markovian dynamics, Sci. Rep. **2**, 968 (2012).

[63] S. M. Girvin, M. H. Devoret, and R. J. Schoelkopf, Circuit QED and engineering charge-based superconducting qubits, Phys. Scr. **T137**, 014012 (2009).

[64] A. Blais, R. S. Huang, A. Wallraff, S. M. Girvin, and R. J. Schoelkopf, Cavity quantum electrodynamics for superconducting electrical circuits: An architecture for quantum computation, Phys. Rev. A **69**, 062320 (2004).

[65] S. Felicetti, M. Sanz, L. Lamata, G. Romero, G. Johansson, P. Delsing, and E. Solano, Dynamical Casimir Effect Entangles Artificial Atoms, Phys. Rev. Lett. **113**, 093602 (2014).

[66] E. M. Laine, H. P. Breuer, J. Piilo, C. F. Li, and G. C. Guo, Nonlocal Memory Effects in the Dynamics of Open Quantum Systems, Phys. Rev. Lett. **108**, 210402 (2012).

[67] B. H. Liu, D. Y. Cao, Y. F. Huang, C. F. Li, G. C. Guo, E. M. Laine, H. P. Breuer, and J. Piilo, Photonic realization of nonlocal memory effects and non-Markovian quantum probes, Sci. Rep. **3**, 1781 (2013).

[68] G. Y. Xiang, Z. B. Hou, C. F. Li, G. C. Guo, H. P. Breuer, E. M. Laine, and J. Piilo, Entanglement distribution in optical fibers assisted by nonlocal memory effects, Europhys. Lett. **107**, 54006 (2014).

[69] E. M. Laine, H. P. Breuer, and J. Piilo, Nonlocal memory effects allow perfect teleportation with mixed states, Sci. Rep. **4**, 4620 (2014).

[70] S. Blanes, F. Casas, J. A. Oteo, and J. Ros, The Magnus expansion and some of its applications, Phys. Rep. **470**, 151 (2009).

[71] N. Bar-Gill, D. D. Bhaktavatsala Rao, and G. Kurizki, Creating Nonclassical States of Bose-Einstein Condensates by Dephasing Collisions, Phys. Rev. Lett. **107**, 010404 (2011).

[72] J. Łuczka, Spin in contact with thermostat: Exact reduced dynamics, Phys. A **167**, 919 (1990).

[73] G. M. Palma, K. A. Suominen, and A. K. Ekert, Quantum computers and dissipation, Proc. R. Soc. London, Ser. A **452**, 567 (1996).

[74] J. H. Reina, L. Quiroga, and N. F. Johnson, Decoherence of quantum registers, Phys. Rev. A **65**, 032326 (2002).

[75] M. J. Biercuk, H. Uys, A. P. VanDevender, N. Shiga, W. M. Itano, and J. J. Bollinger, Optimized dynamical decoupling in a model quantum memory, Nature (London) **458**, 996 (2009).

[76] M. J. Hartmann, F. G. S. L. Brando, and M. B. Plenio, Strongly interacting polaritons in coupled arrays of cavities, Nat. Phys. **2**, 849 (2006).

[77] G. Romero, D. Ballester, Y. M. Wang, V. Scarani, and E. Solano, Ultrafast Quantum Gates in Circuit QED, Phys. Rev. Lett. **108**, 120501 (2012).

[78] Z. L. Xiang, S. Ashhab, J. Q. You, and F. Nori, Hybrid quantum circuits: Superconducting circuits interacting with other quantum systems, Rev. Mod. Phys. **85**, 623 (2013).

[79] S. L. Zhu, Z. D. Wang, and K. Y. Yang, Quantum-information processing using Josephson junctions coupled through cavities, Phys. Rev. A **68**, 034303 (2003).

[80] J. Q. You and F. Nori, Quantum information processing with superconducting qubits in a microwave field, Phys. Rev. B **68**, 064509 (2003).

[81] Z. Y. Xue and Z. D. Wang, Simple unconventional geometric scenario of one-way quantum computation with superconducting qubits inside a cavity, Phys. Rev. A **75**, 064303 (2007).

[82] Y. B. Gao, Y. D. Wang, and C. P. Sun, Nonlinear mechanism of charge-qubit decoherence in a lossy cavity: Quasi-normal-mode approach, Phys. Rev. A **71**, 032302 (2005).

[83] B. Abdo, A. Kamal, and M. Devoret, Nondegenerate three-wave mixing with the Josephson ring modulator, Phys. Rev. B **87**, 014508 (2013).